

## GMRT Detection of HI 21 cm Associated Absorption towards the $z = 1.2$ Red Quasar 3C 190

C. H. Ishwara-Chandra<sup>1</sup>, K. S. Dwarakanath<sup>2</sup> & K. R. Anantharamaiah<sup>2\*</sup>

<sup>1</sup>National Center for Radio Astrophysics, TIFR, Post Bag 3, Ganeshkhind, Pune 411 007, India. e-mail: ishwar@ncra.tifr.res.in

<sup>2</sup>Raman Research Institute, Sadashivanagar, Bangalore 560 080, India. e-mail: dwaraka@rri.res.in

Received 2003 March 27; accepted 2003 June 5

**Abstract.** We report the GMRT detection of associated HI 21 cm-line absorption in the  $z = 1.1946$  red quasar 3C 190. Most of the absorption is blue-shifted with respect to the systemic redshift. The absorption, at  $\sim 647.7$  MHz, is broad and complex, spanning a velocity width of  $\sim 600$  km s<sup>-1</sup>. Since the core is self-absorbed at this frequency, the absorption is most likely towards the hotspots. Comparison of the radio and deep optical images reveal linear filaments in the optical which overlap with the brighter radio jet towards the south-west. We therefore suggest that most of the HI 21 cm-line absorption could be occurring in the atomic gas shocked by the south-west jet.

**Key words.** Galaxies: active—quasars: absorption lines—radio lines: galaxies—quasars: individual (3C190).

### 1. Introduction

It was suggested more than three decades ago that the study of HI 21 cm-line absorption at high redshifts would provide interesting and important information regarding the distribution and kinematics of neutral hydrogen at earlier epochs (Bahcall & Ekers 1969). The central regions of active galactic nuclei (AGN) are important in understanding many aspects of AGN phenomena like the fueling on to the accretion disk and the obscuration of the nuclei as proposed in the unified scheme. One way to study the central region in AGNs is to search for HI 21 cm-line absorption at the redshift of the AGN host galaxy against the radio source. The absorption can be due to a variety of phenomena like tori, outflows, the inter stellar medium (ISM), cold clouds and cold gas stirred up during merging of neighbors with the host galaxy (cf. Morganti *et al.* 2001).

The red quasars have generated interest particularly since the work of Webster *et al.* (1995) claiming that a large fraction ( $\sim 80\%$ ) of quasars could be missed from optical surveys due to dust extinction. It is believed that in this class of quasars, the extinction

\*Since deceased.

due to dust is higher (Webster *et al.* 1995); however, there are claims that red quasars are not necessarily dusty (e.g., Benn *et al.* 1998). If the red quasars are dusty, then the number of high column density absorption-line systems seen towards optically selected quasars will also be an underestimate. Carilli *et al.* (1998; hereinafter C98) have searched for HI 21 cm-line absorption in a radio-loud red quasar subsample at moderate redshifts ( $z \sim 0.7$ ) to address whether the ‘red’ AGNs are intrinsically red or reddened by dust. In their sample of five red quasars, four showed significant HI absorption, suggesting the presence of large amounts of gas and associated dust. Even though the number is small, this study showed that the success rate for detecting HI 21 cm-line absorption in radio-loud red quasars is higher (80%) compared to an optically selected sample of radio-loud quasars with Mg II or Lyman alpha absorption (C98, Carilli *et al.* 1999). This opens up a new class of objects which can be studied in 21-cm absorption at higher redshifts, where the optically selected sample has strong bias against high column density systems with high dust-to-gas ratios (Fall & Pei 1993, 1995).

We have started a program to search for HI 21 cm-line absorption in a sample of high redshift ( $z > 1$ ) radio-loud ‘red’ quasars and galaxies with the Giant Meterwave Radio Telescope (GMRT, Swarup *et al.* 1991). At higher redshifts, the optical/IR morphologies of the host galaxies tend to be more complex, possibly due to ongoing merging activity leading to the formation of massive ellipticals at later epochs (Chambers & Miley 1990). Such activity (i) might enhance the probability of detecting HI 21 cm-line absorption (e.g., Carilli & van Gorkom 1992) and (ii) could also contribute to reddening.

3C 190 is a compact steep spectrum (CSS) radio source. Its largest angular size is 4.0 arcsec and corresponding linear size is 33 kpc (assuming  $H_0 = 71 \text{ km s}^{-1}$ ,  $\Omega_m = 0.27$  and  $\Omega_{\text{vac}} = 0.73$ ). The bright hotspots are separated by 2.6 arcsec, or a linear size of 22 kpc which means the hotspots may be just within the envelope of the host galaxy (Spencer *et al.* 1991). Compact steep spectrum sources and compact symmetric objects appear to show a high incidence of HI absorption (Conway 1996). High resolution radio observations of 3C 190 suggest one-sided jet-like structure towards the south-west of the core (Spencer *et al.* 1991). The large scale jet in this direction is also brighter. The core is self-absorbed at 608 MHz (Nan Rendong *et al.* 1991). There appears to be significant bending between the milli-arcsec scale jet and the kpc scale jet. The milli-arcsec scale jet is directed towards the west (Hough *et al.* 2002), while on larger scales the jet has bent towards south-west ending with multiple hotspots. The diffuse lobe in this direction is further towards south-west ( $\sim 1.5$  arcsec) and also misaligned (Spencer *et al.* 1991). This is suggestive of the presence of a dense inter stellar medium (ISM) causing the jet to bend. Recent detailed optical spectroscopy of this object showed narrow [O II], [Ne III] and C III] emission lines, which provide a redshift of  $1.1946 \pm 0.0005$  (Stockton & Ridgway 2001). In addition, Mg I, Fe II and strong Mg II absorption has also been detected, but at a slightly higher redshift of  $1.19565 \pm 0.00004$ , corresponding to an infall velocity of  $145 \text{ km s}^{-1}$  in the quasar frame (Stockton & Ridgway 2001). We adopt the redshift of  $1.1946 \pm 0.0005$  determined from narrow emission lines as the systemic redshift of the quasar. Its optical to infrared continuum falls steeply, causing it to be classified as a ‘‘red’’ quasar (Simpson & Rawlings 2000; Smith & Spinrad 1980). The presence of strong Mg II absorption close to the systemic redshift suggests the presence of intervening gas and dust, which may also be responsible for reddening the quasar spectrum and causing the bending

of radio jets. A higher chance of detection of HI 21 cm-line absorption from 3C 190 was foreseen due to two factors: (i) it is a CSS radio source. Associated optical/UV absorption is most common in CSS quasars among radio-loud quasars (Baker *et al.* 2002), and CSS also shows a higher chance of detecting HI 21 cm-line absorption (Conway 1996), (ii) it is also a “red” quasar which again shows a higher chance of detecting HI 21 cm-line absorption (C98).

In this paper, we report the detection of HI 21 cm-line absorption from the red quasar 3C 190, which is blue-shifted with respect to the systemic redshift. In section 2 observations and results are presented. The HI 21 cm-line absorption detected in 3C 190 is discussed in section 3. Conclusions are presented in section 4.

## 2. Observations and results

The observations were carried out using the Giant Meterwave Radio Telescope (GMRT) during September 2001. The first set of observations adopted a bandwidth of 4 MHz centered at 647.5 MHz. Subsequently, two sets of observations each with a bandwidth of 8 MHz centered at 646.7 MHz and 648.7 MHz were repeated to confirm the detection from the first set of observations. The integration time on source was  $\sim 3$  hr in each set of observations. The velocity resolutions were  $\sim 29$  km s $^{-1}$  and  $\sim 14.5$  km s $^{-1}$  for bandwidths of 8 MHz and 4 MHz respectively. The flux densities were estimated by observing the standard primary calibrators 3C 286 or 3C 48. The bandpass calibrators 3C 48, 3C 147 and 3C 286 were observed at the beginning as well as at the end of the observation in order to check for bandpass stability with time. Phase calibrators were observed for 10 minutes every 30 minutes.

The data obtained from the GMRT were converted to FITS and analysed using the Astronomical Image Processing System (AIPS) following standard procedures. About 20 line-free channels were collapsed to obtain a continuum image. A few iterations of phase-only self-calibration were performed followed by amplitude and phase self-calibration. These calibrations were then applied to the spectral line data. The continuum flux density of 3C 190 at 647 MHz is 5.69 Jy. The continuum flux density for subtracting from the spectral data was obtained by averaging several line-free channels. The final spectral cube was made from this continuum subtracted data.

Initially, individual spectra were obtained from the two 8 and one 4 MHz observations to check for consistency. The individual spectra were then averaged to obtain the final spectrum which is presented in Fig. 1. The systemic redshift and the relative velocity of the associated optical absorption system (Stockton & Ridgway 2001) are marked in Fig. 1. The RMS noise in the averaged spectrum is  $\sim 2$  mJy/beam/channel. We have used the standard GIPSY package to fit Gaussians to the observed spectra. A minimum of 5 Gaussians were required to minimise the residuals. The estimated parameters of the fit are given in Table 1.

The most interesting finding from our observations is that most of the HI 21 cm-line absorption in 3C 190 is blue-shifted with respect to the systemic redshift (Fig. 1). The peak of the absorption occurs at a velocity of  $-210$  km s $^{-1}$ , but the overall absorption is very broad, extending from  $-400$  km s $^{-1}$  to  $+200$  km s $^{-1}$ . The velocity uncertainties in systemic redshift is 68 km s $^{-1}$  and that of Mg II absorption system is 5.5 km s $^{-1}$ . The components 1, 2 and 3 are significantly blue-shifted with respect to the systemic redshift, while component 4 is within the uncertainty in the systemic redshift. Component 5 at 127 km s $^{-1}$  is outside the uncertainty in the Mg II absorption system and

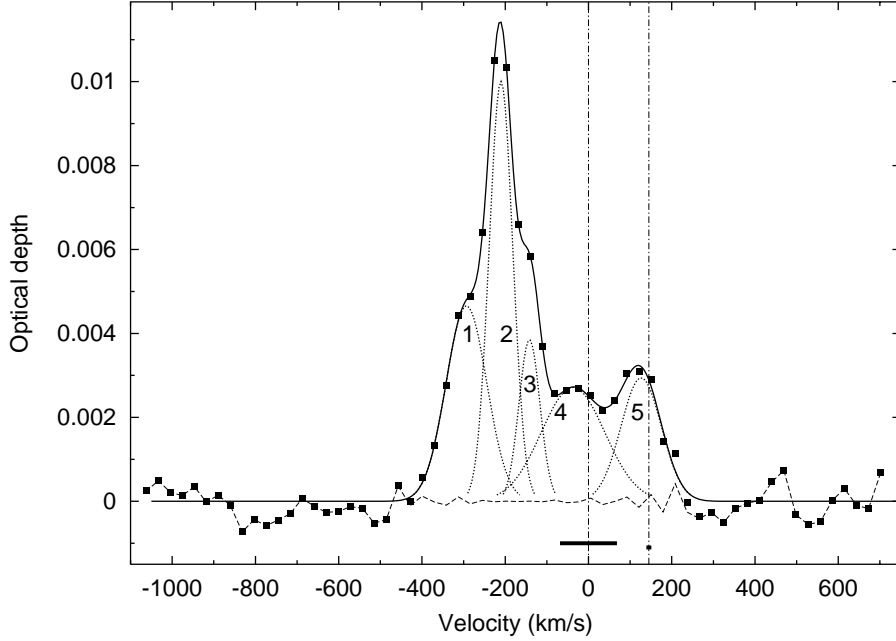


**Figure 1.** The HI absorption spectrum toward the red quasar 3C 190 (indicated by filled squares). The solid line is the five component Gaussian fit to the data and the dotted lines are the individual Gaussian components which are numbered. Dashed line is the residual to the fit. The optical depth was estimated using the peak flux of  $5.69 \text{ Jy}$ . The systemic redshift is taken as  $1.1946 \pm 0.0005$  obtained from narrow [O II], [Ne III] and C III] emission lines, which is indicated as dot-dashed vertical line at the velocity of  $0 \text{ km s}^{-1}$ . Similar vertical line at a velocity of  $145 \text{ km s}^{-1}$  corresponds to the Mg II absorption. Thick horizontal lines centered at  $0$  and  $145 \text{ km s}^{-1}$  indicates one sigma range of velocity at systemic redshift and that at Mg II absorption.

**Table 1.** Parameters derived from the Gaussian fitting to the optical depth profile towards 3C 190. Zero velocity corresponds to the systemic redshift of 1.1946.

Line	Velocity ( $\text{kms}^{-1}$ )	FWHM ( $\text{kms}^{-1}$ )	$\tau$
Comp 1	$-293.1 \pm 2.8$	$115.1 \pm 6.9$	$0.0047 \pm 0.0002$
Comp 2	$-210.2 \pm 1.0$	$66.8 \pm 2.2$	$0.0100 \pm 0.0003$
Comp 3	$-141.8 \pm 2.2$	$59.4 \pm 5.0$	$0.0043 \pm 0.0003$
Comp 4	$-37.1 \pm 5.7$	$179.4 \pm 13.3$	$0.0027 \pm 0.0002$
Comp 5	$126.5 \pm 4.2$	$114.6 \pm 9.8$	$0.0029 \pm 0.0002$

the uncertainty in the systemic redshift. The three blue-shifted lines also have larger optical depths than lines 4 and 5. Component 1 at  $-293 \text{ km s}^{-1}$  has an optical depth of  $\sim 0.005$  and the second component at  $-210 \text{ km s}^{-1}$  has an optical depth of  $\sim 0.01$ . The optical depth of component 3 is comparable to that of component 1, but FWHM is nearly half of component 1. Components 2 and 3 have comparable FWHM, but optical

depth of component 3 is less than half of component 2. The FWHM of fifth component is comparable to component 1, with optical depth nearly half. Component 4 is well within uncertainty in the systemic redshift, and is the broadest of all components with FWHM of  $179 \text{ km s}^{-1}$ .

### 3. Discussion

A few cases of blue-shifted HI 21 cm-line absorption with respect to the systemic redshift are reported in the literature. A nearby CSS ( $z = 0.06393$ ) PKS B1814–63, exhibits an HI absorption spectrum similar to that seen in 3C 190, viz., a broad shallow feature and blue-shifted deep absorption (Morganti *et al.* 2001). A similar absorption profile is also seen in the radio galaxy 4C 12.50 (Mirabel 1989) where the overall absorption extends over  $900 \text{ km s}^{-1}$ . Another compact radio galaxy, 3C 459, also shows HI absorption blue-shifted with respect to systemic redshift, though weaker than PKS 1814–63 (Morganti *et al.* 2001). The authors suggest that the blue-shift could be due to outflow, possibly associated with the jet/lobes, and the shallow component seen at the systemic redshift is due to a circumnuclear disk. Significantly blue-shifted HI 21 cm-line absorption has also been seen in several Seyfert galaxies. In IC 5063, the HI 21 cm-line absorption is blue-shifted by more than  $600 \text{ km s}^{-1}$  (Oosterloo *et al.* 2000) with respect to the systemic redshift. They suggest that the HI 21 cm-line absorption could be occurring from the gas which has been shocked by the western radio jet. The moderate blue-shift of HI 21 cm-line absorption observed in NGC 1068 and NGC 3079 is suggested to be due to neutral gas participating in the outflow (Gallimore *et al.* 1994).

In the case of 3C 190, the striking aspect is that the HI 21 cm-line absorption is broad and complex and most of the absorption is blue-shifted with respect to systemic redshift (Fig. 1). The total velocity extent is about  $600 \text{ km s}^{-1}$ . The absorption is not against the core because the core is self-absorbed at this frequency. The flux limit for the core is  $< 4 \text{ mJy}$  (Nan Rendong *et al.* 1991), whereas the absorbed flux is up to  $70 \text{ mJy}$ . In the current observations, 3C 190 remains unresolved. In the arcsec resolution map of 3C 190, there are two hotspots in the south-west direction, and are brighter than the north-east hotspot (Spencer *et al.* 1991). The fluxes of individual hotspots are about a Jy and more at 608 MHz (Nan Rendong *et al.* 1991). The total projected extent of hotspots in the south-west and north-east is about 22 kpc, hence these hotspots may lie within the envelope of the host galaxy environment. At this linear scale, there is also evidence for diffuse radio emission (Pearson *et al.* 1985) which is mostly north of the radio core. Significant HI 21 cm-line absorption can occur against one or all of these. The diffuse lobe in the south west is further away (1.5 arcsec) from bright hotspots (Pearson *et al.* 1985), and may lie outside the host galaxy, hence it is less likely to expect HI 21 cm-line absorption against this diffuse lobe.

Even though it is not possible to say which absorption-line is towards which radio component, we can draw indirect conclusions from the known radio and optical morphologies and properties. From the radio image at arc-sec resolution, we see that the south-west diffuse lobe and the farthest hotspot in this direction are mis-aligned (Spencer *et al.* 1991). The immediate surroundings of 3C 190 have been studied in imaging as well as in spectroscopy in great detail using HST and Keck (Stockton & Ridgway 2001). The most interesting feature revealed from the HST observations is a linear knotty optical filament along north-west, very close to the quasar and overlapping (in projection) with the south-west hotspot. Spectroscopy of the linear filament

reveals interesting features. The [O II] line profile clearly divides into low velocity dispersion ( $\sigma \sim 40 \text{ kms}^{-1}$ ) and high velocity dispersion ( $\sigma \sim 200 \text{ kms}^{-1}$ ) groups. The higher velocity dispersion indicates that the gas might have been shocked in some way by the interaction with the jet thereby increasing the turbulent velocity in this region significantly. In the radio map also, there is evidence for jet bending in this region (Stockton & Ridgway 2001), which indicates the presence of a dense medium.

Thus it appears that the overall environment under which the HI 21 cm-line absorption is occurring in 3C 190 appears to be similar to that of IC 5063, where neutral gas has been shocked by the radio jet. Velocities up to  $500 \text{ kms}^{-1}$  are expected from shocks (Dopita & Sutherland 1995). Due to shocks, the neutral gas could acquire significant bulk motion but the internal velocities might not increase significantly. Such clouds could produce reasonably narrow lines (FWHM  $\sim 100 \text{ kms}^{-1}$  or less), but significantly blue-shifted, such as the lines 1, 2 and 3 in 3C 190 (Table 1), where the FWHM is 115, 67 and  $59 \text{ kms}^{-1}$  respectively, but are blue-shifted by 293, 210 and  $142 \text{ kms}^{-1}$  with respect to the systemic redshift.

The optical linear filament which shows high velocity dispersion gas overlaps (in projection) with the south-west hotspot (Stockton & Ridgway 2001). This is suggestive of interaction of the jet with the dense ambient medium responsible for changing the direction of the jet. Thus we can expect that the three blue-shifted absorption-lines (1, 2 and 3) in 3C 190 could be arising from this region. Only one of the absorption-line component (component 4) in 3C 190 is very broad (FWHM of  $179 \text{ kms}^{-1}$ ). This component is well within the uncertainty in the systemic redshift and could be due to more turbulent gas near the region of interaction of radio jet with the ambient medium. Thus, we suggest that lines 1, 2, 3 and 4 are likely to be against the south-west hotspots. The fifth line has a velocity of  $127 \text{ kms}^{-1}$ , which is outside the uncertainty of Mg II absorption system and the uncertainty in the systemic redshift. Since the FWHM of this line is not too narrow ( $115 \text{ kms}^{-1}$ ), it could be from the ISM of the host galaxy.

#### 4. Conclusions

We have reported the GMRT detection of HI 21 cm-line absorption in the  $z = 1.1946$  red quasar 3C 190. The absorption, with peak at  $\sim 647.7 \text{ MHz}$ , is broad and complex, spanning a velocity width of  $\sim 600 \text{ kms}^{-1}$ . Most of the absorption is blue-shifted with respect to the systemic redshift. 3C 190 is unresolved with the present observations. Since the core is self-absorbed at this frequency the absorption must be towards the hotspots. Comparison of the radio and deep optical images reveals linear filaments in the optical which overlap with the brighter radio jet in the south-west direction. We therefore suggest that the blue-shifted HI 21 cm-line absorption could be occurring in the atomic gas shocked by the south-west jet.

#### Acknowledgements

We thank Rajaram Nityananda, Jayaram Chengalur and Chris Carilli for comments on the manuscript. We thank the referee for meticulously reading the manuscript and for constructive suggestions. We thank the staff of the GMRT that made these observations possible. GMRT is run by the National Center for Radio Astrophysics of the Tata Institute of Fundamental Research. This research has made use of the NASA/IPAC

Extragalactic Database (NED) which is operated by the Jet Propulsion Laboratory, California Institute of Technology, under contract with the National Aeronautics and Space Administration (NASA).

### References

- Bahcall, J. N., Ekers, R. D. 1969, *Astrophys. J.*, **157**, 1055.
- Baker, J. C., Hunstead, R. W., Athreya, R. M., Barthel, P. D., de Silva, E., Lehnert, M. D., Saunders, R. D. E. 2002, *Astrophys. J.*, **568**, 592.
- Benn, C. R., Vigotti, M., Carballo, R., Gonzalez-Serrano, J. I., Sánchez, S. F. 1998, *MNRAS*, **295**, 451.
- Carilli, C. L., van Gorkom, J. H. 1992, *Astrophys. J.*, **399**, 373.
- Carilli, C. L., Menten, K. M., Reid, M. J., Rupen, M. P., Yun, M. S. 1998, *Astrophys. J.*, **494**, 175.
- Carilli, C. L., Menten, K. M., Moore, C. P. 1999, in *Highly redshifted radio lines*, (eds.) C. L. Carilli, S. J. E. Radford, K. M. Menten, G. I. Langston, ASP Conference Series, Vol. 156, p. 171.
- Chambers, K. C., Miley, G. K. 1990, in *The Evolution of the Universe of Galaxies*, (eds.) R. G. Kron, ASP Conference Series, Vol. 10, p. 373.
- Conway, J. E. 1996, in *The second workshop on Gigahertz Peaked Spectrum and Compact Steep Spectrum Radio Sources*, (eds.) I. A. G. Snellen, R. T. Schilizzi, H. J. A. Rottgering, M. N. Bremer, Leiden Observatory, p. 98.
- Dopita, M. A., Sutherland, R. S. 1995, *Astrophys. J.*, **455**, 468.
- Fall, S. M., Pei, Y. C. 1993, *Astrophys. J.*, **402**, 479.
- Fall, S. M., Pei, Y. C. 1995, in *QSO Absorption Lines*, (eds.) G. Meylan, (Berlin Heidelberg: Springer-Verlag) p. 23.
- Gallimore, J. F., Baum, S. A., O’Dea, C. P., Brinks, E., Pedlar, A. 1994, *ApJL*, **422**, L13.
- Hough, D. H., Vermeulen, R. C., Readhead, A. C. S., Cross, L. L., Barth, E. L., Yu, L. H., Beyer, P. J., Phifer, E. M. 2002, *Astr. J.*, **123**, 1258.
- Mirabel, I. F. 1989, *Astrophys. J.*, **340**, L13.
- Morganti, R., Oosterloo, T. A., Tadhunter, C. N., van Moorsel, G., Killeen, N., Wills, K. A. 2001, *MNRAS*, **323**, 331.
- Nan Rendong, Schilizzi, R. T., Fanti, C., Fanti, R. 1991, *Astr. Astrophys.*, **252**, 513.
- Oosterloo, T. A., Morganti, R., Tzioumis, A., Reynolds, J., King, E., McCulloch, P., Tsvetanov, Z. 2000, *Astr. J.*, **119**, 2085.
- Pearson, T. J., Readhead, A. C. S., Perley, R. A., 1985. *Astr. J.*, **90**, 738.
- Simpson, C., Rawlings, S. 2000, *MNRAS*, **317**, 1023.
- Smith, H. E., Spinrad, H. 1980, *Astrophys. J.*, **236**, 419.
- Spencer, R. E., Schilizzi, R. T., Fanti, C., Fanti, R., Parma, P., van Breugel, W. J. M., Venturi, T., Muxlow, T. W. B., Rendong, Nan. 1991, *MNRAS*, **250**, 225.
- Stockton, A., Ridgway, S. E. 2001, *Astrophys. J.*, **554**, 1012.
- Swarup, G., Ananthakrishnan, S., Kapahi, V. K., Rao, A. P., Subrahmanya, C. R., Kulkarni, V. K. 1991, *Curr. Sci.*, **60**, 95.
- Webster, R. L., Francis, P. J., Peterson, B. A., Drinkwater, M. J., Masci, F. J. 1995, *Nature*, **375**, 469.